

Figure S1: 53BP1-mCherry construct validation and DNA damage due to migration through confined spaces. Related to Figure 1. (A) Representative image sequence of a HT1080 fibrosarcoma cell expressing 53BP1-mCherry treated with Phleomycin, showing increasing number of 53BP1-mCherry foci over time, indicating increasing DNA damage. Scale bar: 5 μm **(B)** Percentage of HT1080 cells with new DNA damage (53BP1-mCherry foci) before Phleomycin treatment and after 60 minutes of Phleomycin treatment. $n = 86$ cells; *, $p < 0.05$ based on unpaired t -test with Welch's correction. **(C)** Representative image panel showing co-localization between γ -H2AX foci and 53BP1-mCherry foci in MDA-MB-231 and HT1080 cells. Scale bar: 10 μm **(D)** Percentage of human fibroblast cells with new DNA damage (53BP1-mCherry foci) during migration through small ($\leq 2 \times 5 \mu\text{m}^2$) constrictions ($n = 230$ cells) or $15 \times 5 \mu\text{m}^2$ control channels ($n = 135$ cells). **(E)** Percentage of RPE-1 retinal epithelial cells with new DNA damage (53BP1-mCherry foci) during migration through small ($\leq 2 \times 5 \mu\text{m}^2$) constrictions ($n = 407$ cells) or $15 \times 5 \mu\text{m}^2$ control channels ($n = 259$ cells). *, $p < 0.05$ based on unpaired t -test with Welch's correction. **(F)** Percentage of BT-549 breast cancer cells with new DNA damage (53BP1-mCherry foci) during migration through small ($\leq 2 \times 5 \mu\text{m}^2$) constrictions ($n = 555$ cells) or 15×5

μm^2 control channels ($n = 260$ cells). **, $p < 0.01$ based on unpaired t -test with Welch's correction. **(G)** Percentage of human fibroblasts cells in which new DNA damage during migration through $\leq 2 \times 5 \mu\text{m}^2$ constrictions was associated with either NE rupture or with nuclear deformation in the absence of NE rupture. $n = 230$ cells **(H)** Percentage of RPE-1 cells in which new DNA damage during migration through $\leq 2 \times 5 \mu\text{m}^2$ constrictions was associated with either NE rupture or with nuclear deformation in the absence of NE rupture. $n = 407$ cells; *, $p < 0.05$ based on unpaired t -test with Welch's correction. **(I)** Percentage of BT-549 cells in which new DNA damage during migration through $\leq 2 \times 5 \mu\text{m}^2$ constrictions was associated with either NE rupture or with nuclear deformation in the absence of NE rupture. $n = 555$ cells; *, $p < 0.05$ based on unpaired t -test with Welch's correction. **(J)** Percentage of cells in which new DNA damage during migration through $\leq 2 \times 5 \mu\text{m}^2$ constrictions was associated with either NE rupture (Rupture) or with nuclear deformation in the absence of NE rupture (Deformation), for a panel of cell lines. The results correspond to the data presented in Fig. 1C and 1F, and Suppl. Fig. S1G-I. *, $p < 0.05$; ***, $p < 0.001$ based on unpaired t -test with Welch's correction. **(K)** Migration speed of MDA-MB-231 cells during migration through $\leq 2 \times 5 \mu\text{m}^2$ constrictions in the microfluidic device ($n = 537$ cells) and collagen matrices (1.7 mg/ml of collagen; $n = 27$ cells). Differences were not statistically significant based on Chi-square test. **(L)** Percentage of MDA-MB-231 breast cancer cells with new DNA damage (53BP1-mCherry foci) due to mild ($n = 37$ cells), moderate ($n = 21$ cells), or severe ($n = 19$ cells) nuclear deformation during migration through a collagen matrix (1.7 mg/ml). ***, $p < 0.001$ based on Chi-square test. Data in this figure are presented as mean + S.E.M.

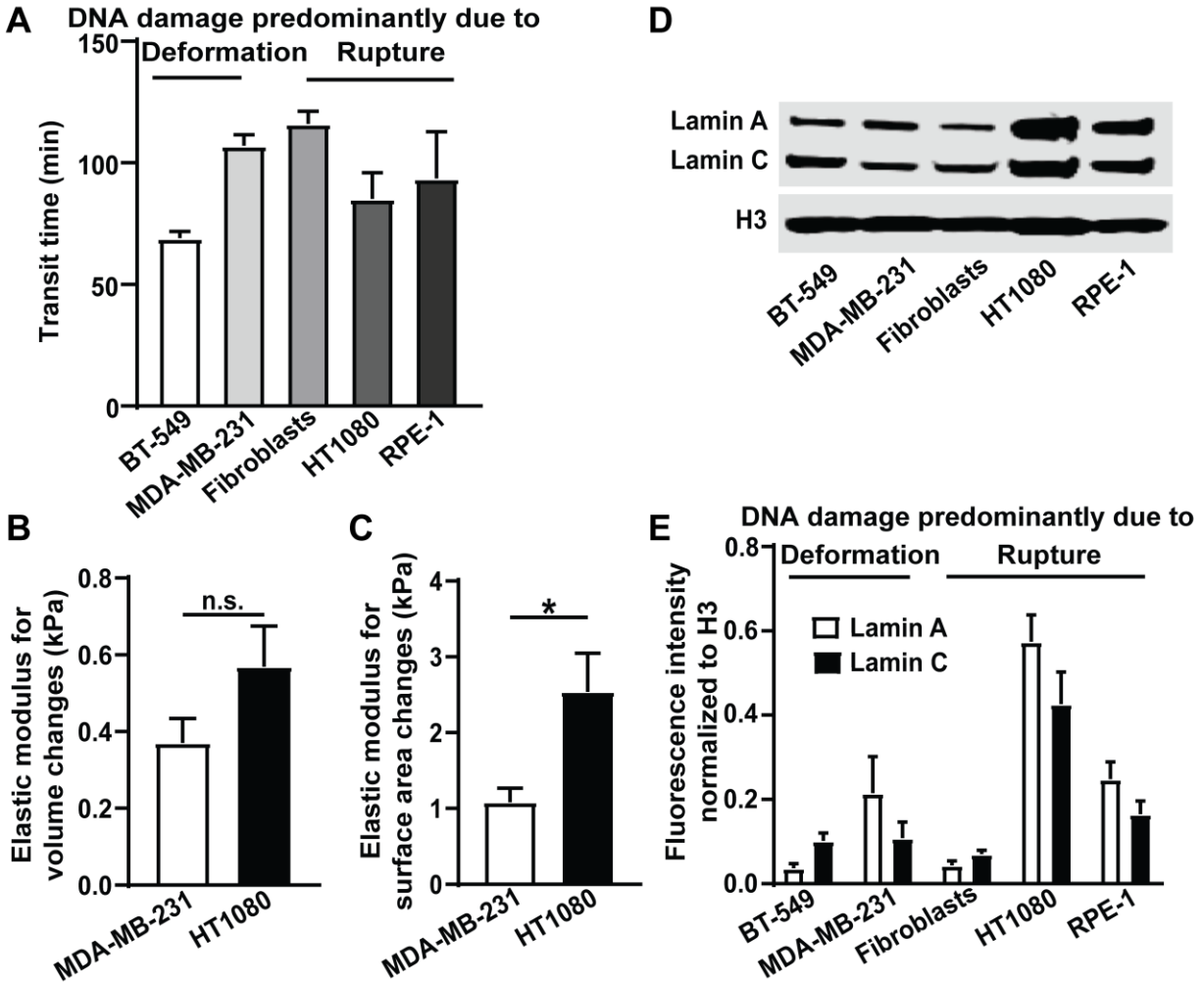


Figure S2: Transit time, nuclear deformability, and lamin A/C level analysis in a panel of cell lines. Related to Figure 1. (A) Transit time for BT-549 ($n = 444$ cells), MDA-MB-231 ($n = 381$ cells), human fibroblasts ($n = 125$ cells), HT1080 ($n = 326$ cells), and RPE-1 ($n = 269$ cells) cells to migrate through $\leq 2 \times 5 \mu\text{m}^2$ constrictions in the microfluidic device. **(B)** Elastic modulus for MDA-MB-231 ($n = 17$ cells) and HT1080 ($n = 15$ cells) cells for bulk nuclear deformation by a beaded AFM tip. Differences were not statistically significant based on unpaired t -test with Welch's correction. **(C)** Elastic modulus for nuclear surface area deformation for MDA-MB-231 ($n = 17$ cells) and HT1080 ($n = 15$ cells) cells probed with a beaded AFM tip. *, $p < 0.05$ based on unpaired t -test with Welch's correction. **(D)** Representative western blot of lamin A and C levels in a panel of human cell lines. Histone H3 was used as a loading control. **(E)** Quantification of lamin A and C levels based on $N = 3$ western blot experiments. Data in this figure are presented as mean + S.E.M.

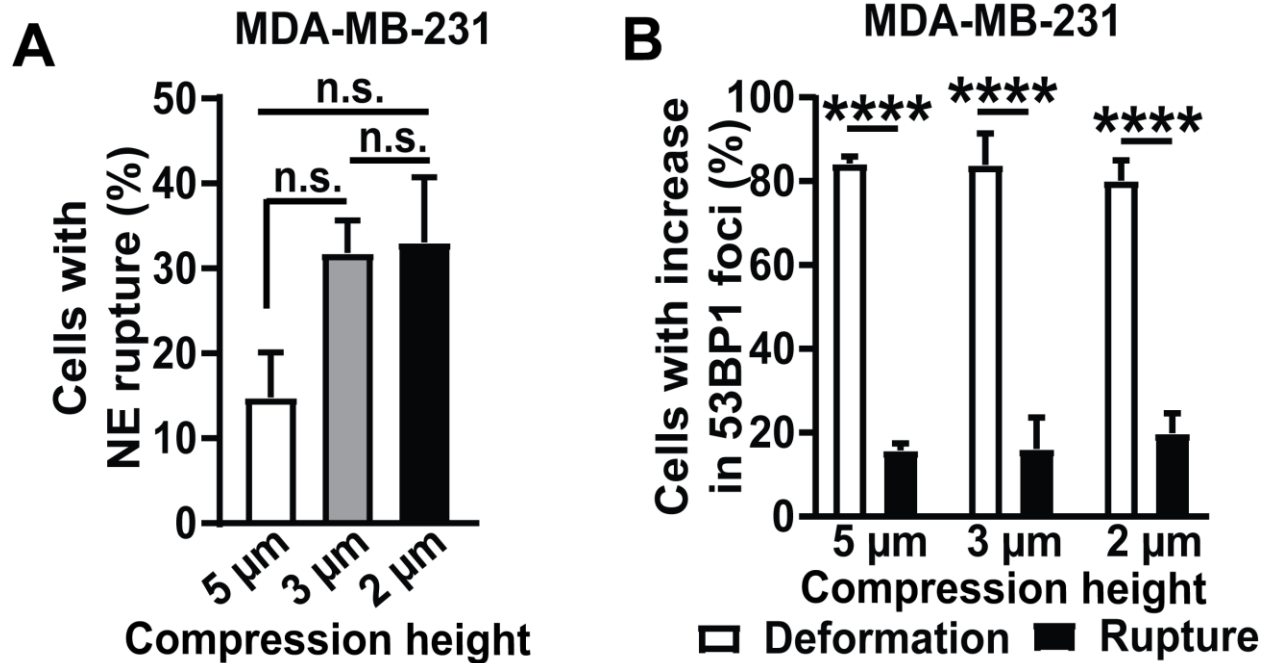


Figure S3: Cell compression causes NE rupture and DNA damage. Related to Figure 2. (A) Percentage of MDA-MB-231 cells that experience NE rupture during external compression to 5 μm height ($n = 500$ cells), 3 μm height ($n = 378$ cells), or 2 μm height ($n = 411$ cells). Differences were not statistically significant based on one-way ANOVA with Dunnett's multiple comparison test. **(B)** Percentage of MDA-MB-231 cells in which new DNA damage during compression to 5 μm , 3 μm , or 2 μm height was associated with either NE rupture or with nuclear deformation without NE rupture. ****, $p < 0.0001$ based on two-way ANOVA with Tukey's multiple comparison test. Data in this figure are presented as mean + S.E.M.

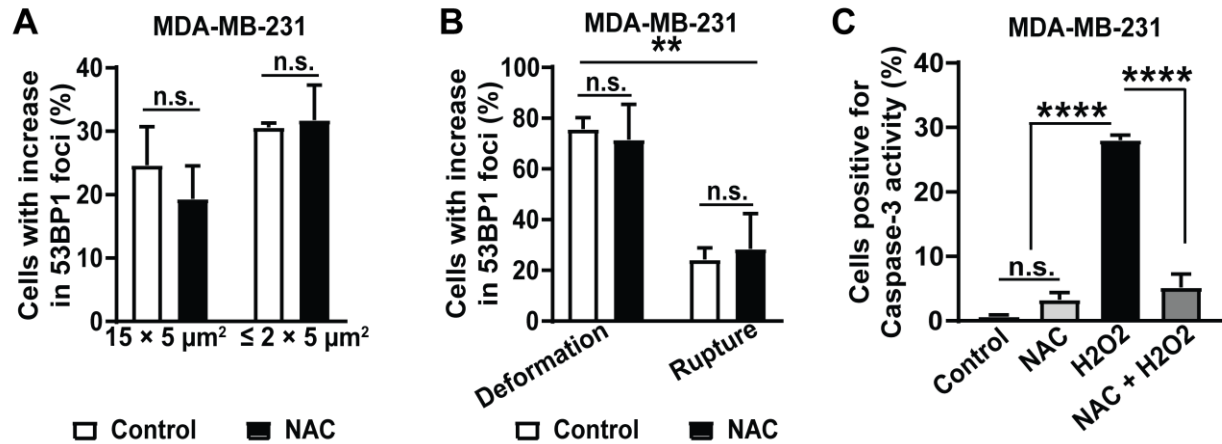


Figure S4: NAC treatment does not rescue DNA damage. Related to Figure 1,2. (A) Percentage of MDA-MB-231 cells treated with or without NAC that exhibit new DNA damage (53BP1-mCherry foci) during migration through small ($\leq 2 \times 5 \mu\text{m}^2$) constrictions ($n = 181$ cells for vehicle control; $n = 182$ cells for NAC treatment) or $15 \times 5 \mu\text{m}^2$ control channels ($n = 95$ cells for vehicle control; $n = 83$ for NAC treatment). Differences were not statistically significant based on two-way ANOVA with Tukey's multiple comparison test. **(B)** Percentage of MDA-MB-231 cells treated with or without NAC in which new DNA damage during migration through small ($\leq 2 \times 5 \mu\text{m}^2$) constrictions was associated with either NE rupture or with nuclear deformation in the absence of NE rupture. **, $p < 0.01$ based on two-way ANOVA with Tukey's multiple comparison test. **(C)** Percentage of MDA-MB-231 cells undergoing apoptosis (positive for Caspase-3 activity) after 24 hours of NAC, H₂O₂ and combined NAC and H₂O₂ treatment. $N = 3$ experiments. ****, $p < 0.0001$ based on one-way ANOVA with Tukey's multiple comparison test. Data in this figure are presented as mean + S.E.M.

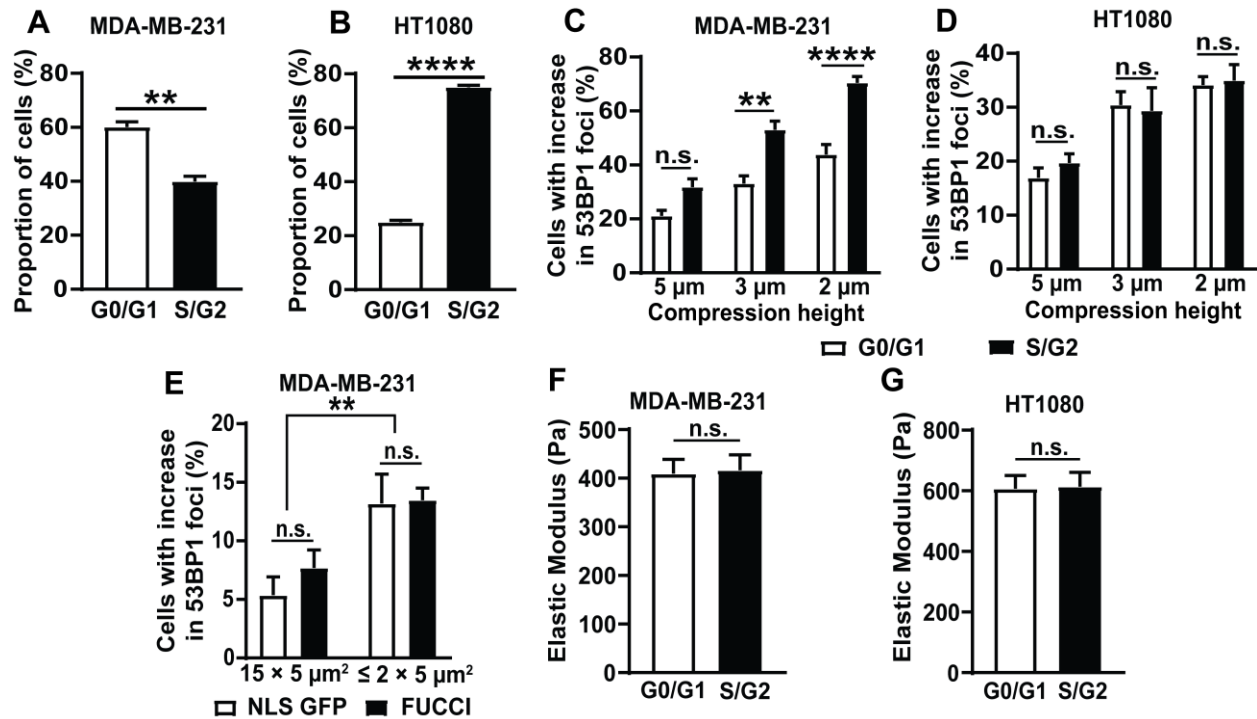


Figure S5: Cell cycle stage analysis by DNA content assay and during nuclear compression. Related to Figure 3. (A) Proportion of MDA-MB-231 cells in G0/G1 phase or S/G2 phase of the cell cycle, determined by DNA content assay. **, $p < 0.01$ based on unpaired t -test with Welch's correction. (B) Proportion of HT1080 cells in G0/G1 phase or S/G2 phase of the cell cycle, determined by DNA content assay. ****, $p < 0.0001$ based on unpaired t -test with Welch's correction. (C) Percentage of MDA-MB-231 cells with new DNA damage (53BP1-mCherry foci) in G0/G1 or S/G2 phase of the cell cycle during compression to either 5 μm ($n = 574$ cells), 3 μm ($n = 359$ cells), or 2 μm ($n = 522$ cells) height. **, $p < 0.01$; ****, $p < 0.0001$ based on two-way ANOVA with Tukey's multiple comparison test. (D) Percentage of HT1080 cells with new DNA damage (53BP1-mCherry foci) in G0/G1 or S/G2 phase of the cell cycle during compression to either 5 μm ($n = 656$ cells), 3 μm ($n = 449$ cells) or 2 μm ($n = 672$ cells) height. Differences were not statistically significant based on two-way ANOVA. (E) Percentage of MDA-MB-231 cells expressing NLS-GFP or FUCCI reporter with new DNA damage (53BP1-mCherry foci) during migration through small $\leq 2 \times 5 \mu\text{m}^2$ constrictions ($n = 381$ for NLS-GFP cells and $n = 327$ for FUCCI cells) or $15 \times 5 \mu\text{m}^2$ control channels ($n = 196$ for NLS-GFP cells and $n = 145$ for FUCCI cells). **, $p < 0.01$ based on two-way ANOVA with Tukey's multiple comparison test. (F) Nuclear elastic modulus, measured by AFM indentation with a spherical tip probe, for MDA-MB-231 cells in G0/G1 ($n = 50$ cells) or S/G2 ($n = 50$ cells) phase of cell cycle. Cell cycle phase was determined based on the FUCCI reporter expressed in these cells. Differences were not statistically significant based on unpaired t -test with Welch's correction. (G) Nuclear bulk elastic modulus for HT1080 cells in G0/G1 ($n = 51$ cells) or S/G2 ($n = 51$ cells) phase of cell cycle. Differences were not statistically significant based on unpaired t -test with Welch's correction. Data in this figure are presented as mean + S.E.M.

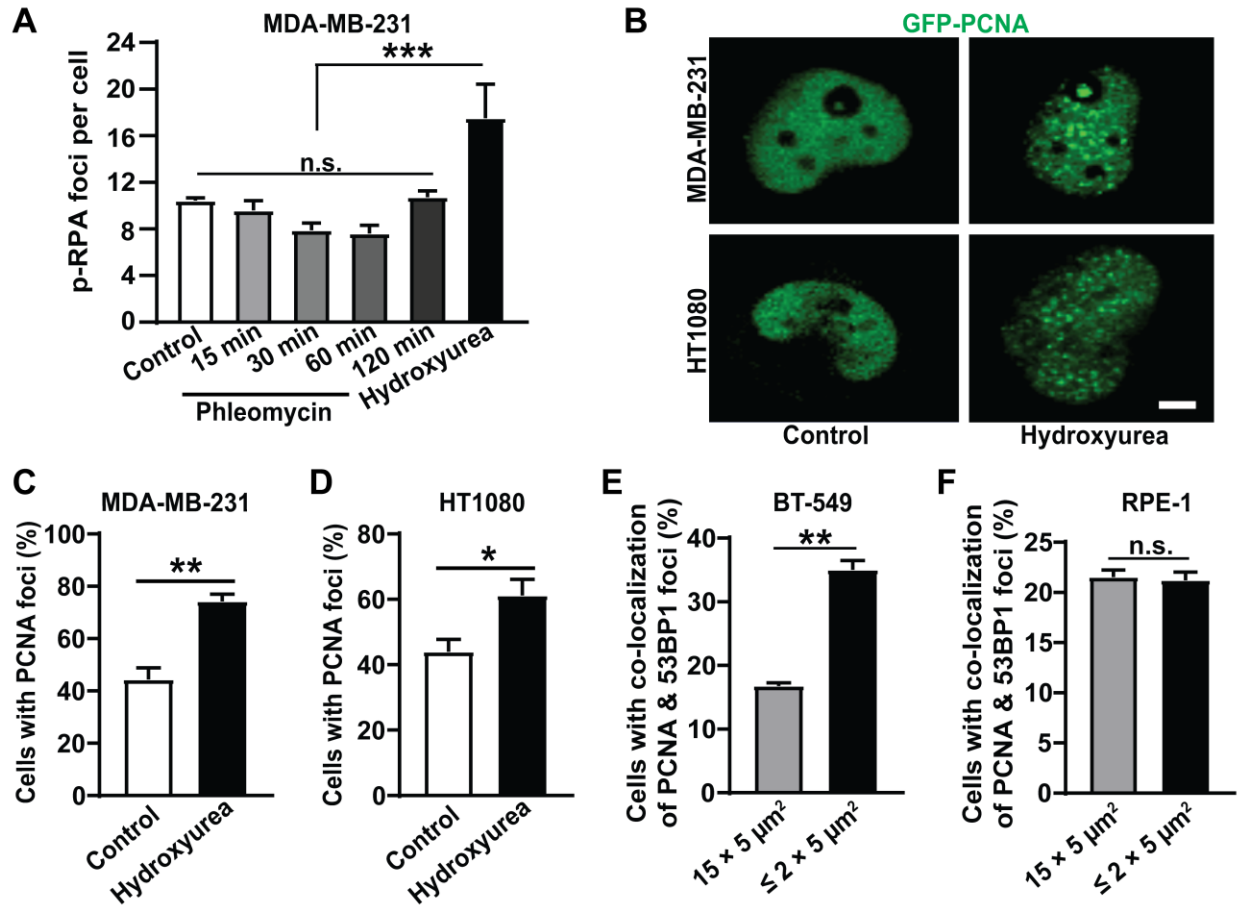


Figure S6: GFP-PCNA construct validation and replication stress experiments. Related to Figure 4. (A) Average number of p-RPA S33 foci in MDA-MB-231 untreated control cells ($n = 235$ cells) or following treatment with Phleomycin for 15 minutes ($n = 201$ cells), 30 minutes ($n = 195$ cells), 60 minutes ($n = 187$ cells), or 120 minutes ($n = 191$ cells). Hydroxyurea treatment (120 minutes) was used as a positive control for replication stress ($n = 158$ cells). $***$, $p < 0.001$ based on one-way ANOVA with Tukey's multiple comparison test. **(B)** Representative image sequence of MDA-MB-231 and HT1080 cells expressing GFP-PCNA, showing an increase in GFP-PCNA foci, indicating stalled replication forks, following treatment with hydroxyurea. Scale bar: $5 \mu\text{m}$. **(C)** Percentage of MDA-MB-231 cells with GFP-PCNA foci following hydroxyurea treatment or vehicle control. $n = 147$ cells for control; $n = 163$ cells for hydroxyurea treatment; $**$, $p < 0.01$ based on unpaired t -test with Welch's correction. **(D)** Percentage of MDA-MB-231 cells with GFP-PCNA foci following hydroxyurea treatment or vehicle control. $n = 132$ cells for control; $n = 143$ cells for hydroxyurea treatment; $*$, $p < 0.05$ based on unpaired t -test with Welch's correction. **(E)** Percentage of BT-549 breast cancer cells with co-localization between new DNA damage (53BP1-mCherry foci) and replication forks (GFP-PCNA foci) during migration through small ($\leq 2 \times 5 \mu\text{m}^2$) constrictions ($n = 154$ cells) or $15 \times 5 \mu\text{m}^2$ control channels ($n = 106$ cells). $**$, $p < 0.01$ based on unpaired t -test with Welch's correction. **(F)** Percentage of RPE-1

retinal epithelial cells with co-localization between new DNA damage (53BP1-mCherry foci) and replication forks (GFP-PCNA foci) during migration through small ($\leq 2 \times 5 \mu\text{m}^2$) constrictions ($n = 249$ cells) or $15 \times 5 \mu\text{m}^2$ control channels ($n = 126$ cells). Differences were not statistically significant based on unpaired t -test. Data in this figure are presented as mean + S.E.M.